J|A|C|S
ARTICLES
Published on Web 12/05/2002

X- and W-Band EPR and Q-Band ENDOR Studies of the Flavin Radical in the Na^+-Translocating NADH:Quinone Oxidoreductase from *Vibrio cholerae*[⊥]

Blanca Barquera,[†] Joel E. Morgan,[†] Dmitriy Lukoyanov,[‡,||] Charles P. Scholes,[‡] Robert B. Gennis,[†] and Mark J. Nilges*[,§]

Contribution from the Department of Biochemistry. University of Illinois at Urbana-Champaign, 600 South Mathews Street, Urbana, Illinois 61801, Illinois EPR Research Center, 506 South Mathews Street, Urbana, Illinois 61801, and Department of Chemistry and Center for Biological Macromolecules, University at Albany, State University of New York, Albany, New York 12222

Received May 22, 2002. Revised Manuscript Received September 23, 2002

Abstract: Na^+-NQR is the entry point for electrons into the respiratory chain of *Vibrio cholerae*. It oxidizes NADH, reduces ubiquinone, and uses the free energy of this redox reaction to translocate sodium across the cell membrane. The enzyme is a membrane complex of six subunits that accommodates a 2Fe−2S center and several flavins. Both the oxidized and reduced forms of Na^+-NQR exhibit a radical EPR signal. Here, we present EPR and ENDOR data that demonstrate that, in both forms of the enzyme, the radical is a flavin semiquinone. In the oxidized enzyme, the radical is a neutral flavin, but in the reduced enzyme the radical is an anionic flavin, where N(5) is deprotonated. By combining results of ENDOR and multifrequency continuous wave EPR, we have made an essentially complete determination of the **g**-matrix and all major nitrogen and proton hyperfine matrices. From careful analysis of the W-band data, the full **g**-matrix of a flavin radical has been determined. For the neutral radical, the **g**-matrix has significant rhombic character, but this is significantly decreased in the anionic radical. The out-of-plane component of the **g**-matrix and the nitrogen hyperfine matrices are found to be noncoincident as a result of puckering of the pyrazine ring. Two possible assignments of the radical signals are considered. The neutral and anionic forms of the radical may each arise from a different flavin cofactor, one of which is converted from semiquinone to flavohydroquinone, while the other goes from flavoquinone to semiquinone, at almost exactly the same redox potential, during reduction of the enzyme. Alternatively, both forms of the radical signal may arise from a single, extremely stable, flavin semiquinone, which becomes deprotonated upon reduction of the enzyme.

Introduction

The Na^+-translocating NADH:quinone oxidoreductase (Na^+-NQR) is an energy-transducing complex that pumps sodium ions across the cell membrane. The enzyme oxidizes NADH, reduces quinone, and uses the free energy released in this redox reaction to generate a sodium motive force that can be used for mobility and metabolic work.[1,2] Na^+-NQR constitutes the entry point for electrons into the aerobic respiratory chain for *Vibrio cholerae*, as well as some other pathogenic and marine bacteria.[3,4]

The typical Na^+-NQR complex is made of six subunits and accommodates several flavins and a 2Fe−2S cluster as prosthetic groups.[5,6] Two flavin cofactors (FMN) are bound covalently to subunits B and C of the enzyme, and another flavin (FAD) is noncovalently bound to subunit F.[7−9] One unusual feature of Na^+-NQR is the presence of a free radical signal, which can be

* To whom correspondence should be addressed. Telephone: (217) 333-3969. Fax: (217) 333-8868. E-mail: m-nilges@uiuc.edu.
[†] University of Illinois at Urbana-Champaign.
[‡] University at Albany, State University of New York.
[§] Illinois EPR Research Center.
[||] On leave from the MRS Laboratory, Kazan State University, 420008, Kazan, Russian Federation.

[⊥] Abbreviations: cw, continuous wave; ptp, peak to peak; i.d., inside diameter; o.d., outside diameter; DM, *n*-dodecyl *β*-maltoside; E_m, midpoint potential; ENDOR, electron nuclear double resonance; EPR, electron paramagnetic resonance; FAD, flavin adenine dinucleotide; Fl•$^-$, anionic flavin radical; FlH•, neutral flavin radical; FMN, flavin adenine mononucleotide; MES, 2-(*N*-morpholino)ethanesulfonic acid; NADH, reduced nicotinamide adenine dinucleotide; NAD^+, nicotinamide adenine dinucleotide; Na^+-NQR, Na^+-translocating NADH:quinone oxidoreductase; Q-1, 2,3-dimethoxy-5-methyl-6-(3-methyl-2-butenyl)-1,4-benzoquinone; rf, radio frequency.

(1) Dibrov, P. A.; Kostyrko, V. A.; Lazarova, R. L.; Skulachev, V. P.; Smirnova, I. A. *Biochim. Biophys. Acta* **1986**, *850*, 449−457.
(2) Unemoto, T.; Akagawa, A.; Hayashi, M. *J. Gen. Microbiol.* **1993**, *139*, 2779−2782.
(3) Kogure, K.; Tokuda, H. *FEBS Lett.* **1989**, *256*, 147−149.
(4) Barquera, B.; Hellwig, P.; Zhou, W.; Morgan, J. E.; Häse, C. C.; Gosink, K.; Nilges, M.; Bruesehoff, P. J.; Roth, A.; Lancaster, C. R. D.; Gennis, R. B. *Biochemistry* **2002**, *41*, 3781−3789.
(5) Bogachev, A. V.; Bertsova, Y. V.; Barquera, B.; Verkhovsky, M. I. *Biochemistry* **2001**, *40*, 7318−7323.
(6) Hayashi, M.; Nakayama, Y.; Unemoto, T. *Biochim. Biophys. Acta* **2001**, *1505*, 37−44.
(7) Hayashi, M.; Nakayama, Y.; Yasui, M.; Maeda, M.; Furuishi, K.; Unemoto, T. *FEBS Lett.* **2001**, *488*, 5−8.
(8) Nakayama, Y.; Yasui, M.; Sugahara, K.; Hayashi, M.; Unemoto, T. *FEBS Lett.* **2000**, *474*, 165−168.
(9) Barquera, B.; Häse, C. C.; Gennis, R. B. *FEBS Lett* **2001**, *492*, 45−49.

Scheme 1. Structures of Anionic and Neutral Flavin Radicals[a]

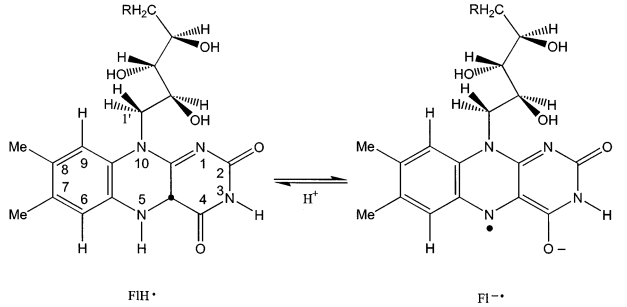

[a] Ring numbering systems are according to IUPAC−IUB nomenclature rules (see ref 41).

detected by EPR in both the oxidized and the reduced forms of the enzyme. Previously, it was reported that this radical was that of an ubi-semiquinone.[10] However, we recently presented evidence that the radical in Na^+-NQR is a flavin semiquinone.[4]

Flavin cofactors are versatile since they can occupy three redox states: oxidized, flavin semiquinone form (one electron reduced) and fully reduced.[11] This property allows flavins to provide an interface between one-electron and two-electron carriers. Flavin semiquinone radicals can be stabilized in their neutral (FlH•) and/or anionic ($Fl•^-$) forms (See Scheme 1), and therefore their structure and interaction with the surrounding protein are keys to understanding their role in overall catalysis.

Flavin semiquinones have been extensively studied by EPR and ENDOR spectroscopies; in particular, proton and nitrogen hyperfine structure has been used to determine the nature of the flavin radical as well as its interaction with surrounding amino acids within the protein.[12,13]

In this paper, we present further EPR and ENDOR data, showing conclusively that the radical signals present in the oxidized and reduced forms of Na^+-NQR are both flavin semiquinones. In the oxidized enzyme, the radical is a neutral semiquinone, but in the reduced enzyme, the radical is an anionic semiquinone.

It is possible that the two forms of the radical arise from two different flavin cofactors, one of which is a semiquinone in the oxidized enzyme and the other is in the reduced enzyme. The data are also consistent with the possibility that the radical in Na^+-NQR is due to a single stable flavin semiquinone, which loses the proton at the N(5) position of the isoalloxazine ring when the enzyme is reduced. For such a proton removal to occur, the flavin would have to be close to a group that takes up a proton. This single-flavin explanation is interesting because it suggests a possible connection between the changes seen in the radical signal and sodium translocation by the enzyme.

Material and Methods

Bacterial Growth and Na^+-NQR Purification. *Vibrio cholerae* cells expressing the recombinant Na^+-NQR were grown in LB medium, as reported before, or in Celtone-N medium (^{15}N-rich medium, isotope enrichment of >98%), obtained from Stable Isotope Biochemicals. Cells obtained from both media yield the same amount of recombinant Na^+-NQR, as confirmed by Western blotting using antibodies against the 6X-His tag. Recombinant Na^+-NQR was purified as reported earlier.[4]

Solvent Exchange. Protein was exchanged with D_2O-containing buffer or aqueous buffers at other pH values by repeated dialysis using BioDialyzers dialysis cells (Harvard Bioscience). At least four changes of buffer were performed at 4 °C. The following buffers were used: pH 6, 50 mM MES, 100 mM NaCl, 0.1% DM, 5% glycerol; pH 7, 50 mM Na phosphate, 100 mM NaCl, 0.1% DM, 5% glycerol. For D_2O buffers: pD 7, 50 mM Na phosphate, (pD = [pH meter reading] + 0.4), 100 mM NaCl, 0.1% DM, 5% glycerol. To adjust pD, DCl and NaOD were used.

EPR Sample Preparation. Enzyme concentration was 150 μM for most of the experiments and 300 μM for W-band EPR. Air-oxidized samples were prepared using the enzyme as isolated and rapidly frozen in liquid nitrogen. Air-oxidized samples were also prepared with NAD^+ also added at a concentration of 1 mM. Na^+-NQR was reduced anaerobically by NADH or by dithionite using a vacuum line or a glovebox. NADH solutions were made air-free by bubbling with nitrogen gas and injected into the samples at two different concentrations, 200 μM and 10 mM. Dithionite was added in a final concentration of 60 mM (in 1 M phosphate buffer, pH 8).

EPR and ENDOR Conditions. Electron paramagnetic resonance experiments were performed at X-band (9.08 GHz) on a Varian E-122 X-band spectrometer. Unless otherwise noted, a microwave power of 0.2 mW was used, with a modulation amplitude of 2.0 G at 100 kHz. Samples were run as frozen glasses at 50 K in 3 mm i.d. tubes using an Air Products Helitran cryostat. The magnetic field was calibrated with a Varian NMR Gaussmeter, and the microwave frequency was determined with an EIP frequency meter (San Jose, CA).

W-band (94 GHz) spectra were obtained on the MARK II W-band EPR spectrometer[14] at the Illinois EPR Research Center (IERC), University of Illinois at Urbana-Champaign, using a modulation amplitude of 2.0 G at 95 kHz. Samples were run as frozen glasses at 100 K in 0.57 mm i.d. tubes using an Oxford CF 1200 cryostat. The magnetic field calibration was obtained by use of a Metrolab PT 2025 NMR Gaussmeter, and the microwave frequency was measured with an EIP Model 578 frequency counter equipped with a high-frequency option. The magnetic field was cross-calibrated using perdeuterated tempone in water as a standard (g = 2.005 51). The use of a 95 GHz low-noise preamplifier (Millitech) allows us to achieve high signal-to-noise ratio at the low microwave powers needed to avoid saturation of the EPR signal.

Q-band (34 GHz) ENDOR measurements were performed at 1.9 K with a cryogenically tunable TE_{011} Q-band resonator[15] located in an immersion double Dewar (Janis, Inc., Wilmington, MA) which was filled with pumped liquid helium. Samples were run as frozen glasses in 2.0 mm i.d. quartz sample tubes. ENDOR was obtained under rapid passage (χ') conditions with 100 kHz field modulation.[16] Features within $\sim \pm 5$ MHz of the free proton frequency are better resolved with a smaller field modulation of 1.2 G ptp, while larger couplings are better resolved with a larger field modulation of 2.4 G ptp. The ENDOR rf field typically had a ptp amplitude of 1 G. The microwave power was ~0.2 μW. For proton ENDOR spectra, one expects two lines for each magnetic nucleus to appear symmetrically spaced, to first order, about the nuclear Larmor frequency, ν_H, and separated by the respective proton hyperfine coupling, A. The ENDOR frequencies ν_{ENDOR} are given by $\nu_{ENDOR}^{\pm} = |\nu_H \pm A/2|$. EPR frequencies were measured with an EIP Model 548 microwave frequency counter (San Jose, CA); g values were calibrated versus a DPPH (2,2-diphenyl-1-picrylhydrazyl, Sigma) sample having a known g value of 2.0036.

(10) Pfenninger-Li, X. D.; Albracht, S. P. J.; van Belzen, R.; Dimroth, P. *Biochemistry* **1996**, *35*, 6233−6242.
(11) Massey, V. *Biochem. Soc. Trans.* **2000**, *28*, 283−296.
(12) Galli, C.; MacArthur, R.; Abu-Soud, H. M.; Clark, P.; Stuehr, D. J.; Brudvig, G. W. *Biochemistry* **1996**, *35*, 2804−2810.
(13) Kay, C. W. M.; Feicht, R.; Schulz, K.; Sadewater, P.; Sancar, P.; Bacher, A.; Möbius, K.; Richter, G.; Weber, S. *Biochemistry* **1999**, *38*, 16740−16748.
(14) Nilges, M. J.; Smirnov, A. I.; Clarkson, R. B.; Belford, R. L. *Appl. Magn. Res.* **1999**, *16*, 167−183.
(15) Sienkiewicz, A.; Smith, B. G.; Veselov, A.; Scholes, C. P. *Rev. Sci. Instrum.* **1996**, *67*, 2134−2138.
(16) Scholes, C. P.; Falkowski, K. M.; Chen, S.; Bank, J. *J. Am. Chem. Soc.* **1986**, *108*, 1660−1671.

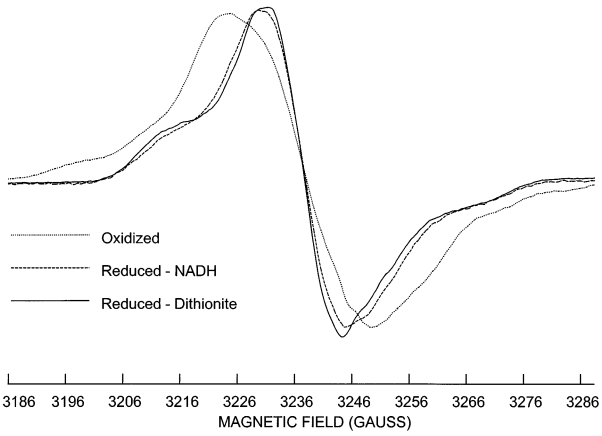

Figure 1. First-derivative X-band spectra of Na^+-NQR: dotted, oxidizing conditions; dashed, reduced with 200 μM NADH; solid line, reduced with 60 mM dithionite.

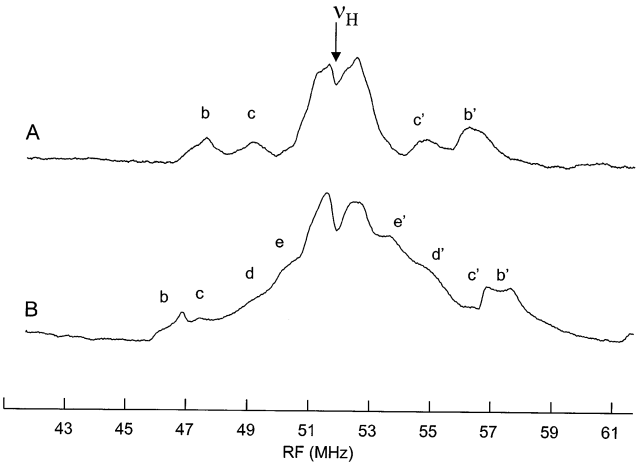

Figure 2. Q-band ENDOR spectra comparing proton features from Na^+-NQR prepared under oxidizing conditions (A) and dithionite-reduced conditions (B) over a wide frequency range of 20 MHz centered at the free proton frequency, ν_H. Features b and b′ are assigned to the C(8)-methyl protons. (Conditions were $T = 1.9$ K, microwave power = 0.24 μW, field modulation 1 G ptp, rf power about 20 W pulsed with 10% duty cycle, $\nu_e = 34.080$ GHz, $B = 12\,154$ G, $g = 2.0033$, frequency sweep rate 2 MHz/s, experimental time constant 0.08 s, and each spectrum was the average of 30 traces, each taking 10 s.)

Simulation of electron paramagnetic resonance spectra used the automated simulation program SIMPOW6 (Nilges, ftp://ierc.scs.uiuc.edu), which is based upon POW.[17] This program generates a powder spectrum for a spin 1/2 system with two hyperfine terms calculated to second order (in this case the two nitrogen splittings) and four hyperfine spins calculated to first order. The program uses the Simplex algorithm to minimize the square difference (SD) between the experimental and simulated spectra. In the case of multifrequency and/or multi-isotope spectra, a global simultaneous fitting of the spectra was performed by minimizing the total square difference (TSD). Second-and third-derivative spectra were obtained numerically with DATAEG (Nilges, ftp://ierc.scs.uiuc.edu) which employs the regression algorithms of Savitzky et al.[18]

Results

Na^+-NQR in its resting, air-oxidized, form gives rise to a radical EPR signal centered at $g = 2.0036$. When a reductant is added, a nearly axial ($g = 2.0182$, 1.9371, and 1.9316) signal from a reduced 2Fe−2S center appears, but a radical signal is still observed. We have reported[4] the assignment of the radical signal at $g = 2.0036$ as that of a flavin semiquinone.

The X-band EPR spectrum of the air-oxidized enzyme is shown in Figure 1 (dotted line). From the line width of 20.0 G and the shoulders in the wings (^{14}N parallel hyperfine splitting), the signal can be assigned to a neutral flavin radical. For such a radical, significant narrowing to the central feature of the signal (by 6−8 G) would be expected[19,20] in D_2O as a result of exchange of the N(5) proton with a deuteron. However, prolonged incubation in D_2O did not produce any observable change in the EPR spectrum. One would also expect some narrowing at higher pHs, as the pK_a of the N(5) is predicted to be around 8.[19,21] Again, no change in the EPR spectrum is observed over the range of pH 5.5−8.5. Thus, the flavin which gives rise to this EPR signal must be thoroughly isolated from protonic contact with the external medium. While the radical is at or near stoichiometric levels in the air-oxidized enzyme, a 33% decrease in radical signal intensity is observed when the enzyme is incubated in 1 mM NAD^+.

When the enzyme is subjected to reducing conditions, the flavin radical signal changes, but is not eliminated as would be expected. (In fact, the radical signal is only abolished on denaturation of the enzyme.) Even after reduction of the enzyme with NADH, the radical signal is still at stoichiometric levels (1:1 ratio of radical to 2Fe−2S signal), though the signal narrows from 20.0 to 15.3 G. Reduction with sodium dithionite at a 400-fold excess concentration gives a slightly narrower signal (13.3 G) and some decrease in signal intensity (0.85:1 ratio of radical to 2Fe−2S signals). Reoxidation of the enzyme leads to a spectrum identical to that of the initial air-oxidized enzyme. EPR results were the same whether the enzyme was reduced in the presence or absence of O_2, although samples reduced in the absence of O_2 were found to be more stable toward reoxidation (as observed by a decrease in the 2Fe−2S EPR signal). The decrease in line width indicates that, in the reduced enzyme, the radical is deprotonated and, while the deprotonated form is present in the NADH-reduced enzyme, it predominates in the enzyme reduced with an excess of dithionite.

To understand the effects of reducing the sample on the EPR spectrum and to confirm our assignments, we have performed detailed analysis of X-band and W-band spectra and of Q-band ENDOR spectra from the air-oxidized and reduced forms of Na^+-NQR. Because preliminary analysis of the EPR spectrum of NADH-reduced Na^+-NQR indicated that this system is in a partially deprotonated or mixed protonation state, we have focused on the analysis of the spectra of the dithionite-reduced enzyme.

Q-Band ENDOR. ENDOR spectra were taken to resolve proton features that distinguish between the neutral and anionic forms of the flavin radical. Our method of obtaining ENDOR by dispersion rapid passage (χ') generally leads to an absorption-like spectrum. Figure 2 shows proton ENDOR spectra of the radical at 2 K, taken over a 20 MHz range centered at ν_H, comparing a Na^+-NQR sample prepared under oxidizing condi-

(17) Nilges, M. J. Thesis, University of Illinois at Urbana-Champaign: Urbana-Champaign, 1979.
(18) Savitzky, A.; Golay, M. J. E. *Anal. Biochem.* **1964**, *36*, 1627−1639.
(19) Edmondson, D. E. In *Biological Magnetic Resonance*; Berliner, L. J., Reuben, J., Eds.; Plenum Press: New York, 1978; Vol. 1.
(20) Bretz, N. H.; Henzel, N.; Kurreck, H.; Mueller, F. *Isr. J. Chem.* **1989**, *29*, 49−55.
(21) Eriksson, L. E. G.; Ehrenberg, A. *Biochim. Biophys. Acta* **1973**, *293*, 57−66.

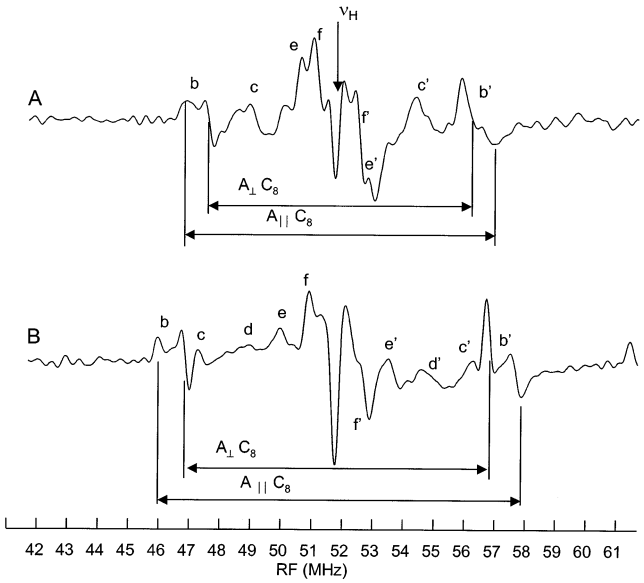

Figure 3. Derivative Q-band ENDOR spectra corresponding to Figure 2 which compare proton features from Na^+-NQR prepared under oxidizing conditions (A) and dithionite-reduced conditions (B) over a frequency range of 20 MHz centered at the free proton frequency, ν_H. Features b and b′ are assigned to the C(8)-methyl protons.

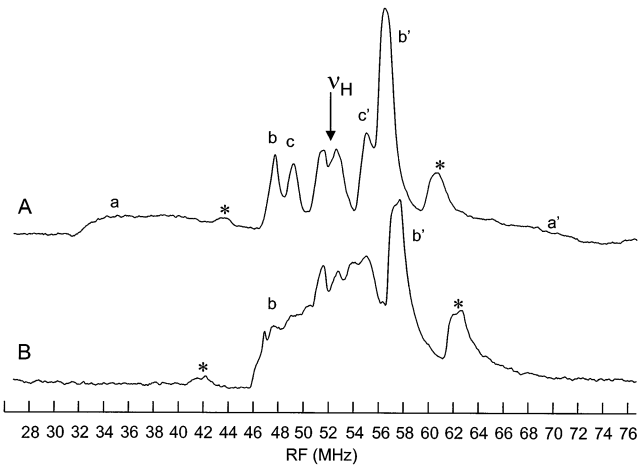

Figure 4. Q-band ENDOR spectra comparing proton features from Na^+-NQR prepared under oxidizing conditions (A) and dithionite-reduced conditions (B) over a frequency range of 50 MHz centered at the free proton frequency, ν_H. Features b and b′ are assigned to the C(8)-methyl protons and a and a′ to the N(5) proton. (Conditions were $T = 1.9$ K, microwave power = 0.24 μW, field modulation 2 G ptp, rf power about 20 W pulsed with 10% duty cycle, $\nu_e = 34.080$ GHz, $B = 12\,154$ G, $g = 2.0033$, frequency sweep rate 2.5 MHz/s, experimental time constant 0.08 s, and each spectrum was the average of 30 traces, each taking 20 s.)

Table 1. ENDOR Hyperfine Couplings for Flavin Protons in Oxidized and Reduced Na^+-NQR

position	oxidized form coupling (MHz)	reduced form coupling (MHz)	feature in figures
N(5)H	35.5 ± 5		a, a′
C(8α)H	$A_{\|\|} = 10.0 \pm 0.1$	$A_{\|\|} = 11.9 \pm 0.1$	b, b′
	$A_\perp = 8.5 \pm 0.1$	$A_\perp = 9.9 \pm 0.1$	
C(6)H	5.7 ± 0.1	8.9 ± 0.1	c, c′
C(1′)H	a	5.9 ± 0.4	d, d′
C(9)H	2.2 ± 0.1	3.6 ± 0.1	e, e′
C(7α)H	1.3 ± 0.1	1.7 ± 0.1	f, f′

[a] Not observed; obscured by C(8) methyl splittings.

tions (A) with one prepared under reducing conditions (B). The most notable difference is in the splitting of the pair of peaks labeled b and b′ in both the oxidized and dithionite-reduced samples. The former has couplings of 8−10 MHz and the latter of 10−12 MHz. These values are consistent with the expected difference for the C(8)-methyl protons, where couplings are typically <10 MHz for a neutral radical and >10 MHz for an anion radical.[21−24]

The numerically calculated derivative spectra corresponding to Figure 2A and 2B are shown in Figure 3A and 3B, respectively. The derivative spectra reveal an axial character in the hyperfine couplings: $A_\perp = 8.5$ and $A_{||} = 10.0$ MHz under oxidizing conditions and $A_\perp = 10.0$ and $A_{||} = 11.9$ MHz for reducing conditions (see Table 1).

At the temperatures where the EPR spectra were acquired (50−100 K), the methyl groups still rotate freely and an average hyperfine splitting is observed for the three protons. The isotropic hyperfine splitting is a result primarily of hyperconjugation:

$$A_{iso} = B_0 + B_2 \cos^2 \theta$$

where θ is the dihedral angle between the p_z orbital on the C(8) atom and the C(8α)−H bond, and as such, the observed averaged methyl splitting is a measure of $B_2/2$, since B_0 is small. In the ENDOR spectra of the enzyme under either oxidizing or reducing conditions, additional peaks (marked * in Figure 4) are seen, corresponding to splittings of 17 and 20 MHz, respectively. This interaction would be expected to also manifest itself as hyperfine structure in the EPR spectra, with splittings of 6 and 7 G, respectively. Such hyperfine structure is not seen in, and is incompatible with, the X- and W-band cw spectra. It is worth noting, however, that the splittings of these extra peaks are 1.9 times the corresponding isotropic values for the C(8)-methyl protons. The appearance of these peaks is probably due to the fact that the ENDOR was run at 2 K, rather than at 50 K for the EPR. Apparently, at 2 K, the temperature is low enough that the methyl groups are partially locked, with one proton having a dihedral angle, θ, near zero, resulting in a value of A_{iso} for this proton slightly less than B_2 or twice the average methyl proton splitting. We have observed similar phenomena previously.[25] ENDOR spectra were also recorded at 80 K (not shown). Although at this temperature the signals for dispersion ENDOR are extremely weak,[25] the oxidized Na^+-NQR showed proton ENDOR features with a coupling of 8.7 ± 0.5 MHz, while the reduced enzyme showed features with a coupling of 11.0 ± 0.9 MHz.

Like the C(8)-methyl protons, the proton at the C(6) position is expected to experience an increase in spin density upon removal of the N(5) proton.[23] Based upon ENDOR studies of substituted lumiflavins, a splitting of 8−11 MHz is expected,[26,27] which would place the peaks for this proton close to, or

(22) Kurreck, H.; Bock, M.; Bretz, N.; Elsner, M.; Kraus, H.; Lubitz, W.; Mueller, F.; Geissler, J.; Kroneck, P. M. H. *J. Am. Chem. Soc.* **1984**, *106*, 737−746.
(23) Edmondson, D. E. *Biochem. Soc. Trans.* **1985**, *13*, 593−600.
(24) Bretz, N. H.; Henzel, N.; Kurreck, H.; Mueller, F. *Isr. J. Chem.* **1989**, *29*, 49−55.
(25) Veselov, A. V.; Osborne, J. P.; Gennis, R. B.; Scholes, C. P. *Biochemistry* **2000**, *39*, 3169−3175.
(26) Eriksson, L. E. G.; Hyde, J. S.; Ehrenberg, A. *Biochim. Biophys. Acta* **1969**, *192*, 211−230.
(27) Müller, F.; Hemmerich, P.; Ehrenberg, A.; Palmer, G.; Massey, V. *Eur. J. Biochem.* **1970**, *14*, 185−196.

overlapping with, those for C(8)-methyl protons.[21,23] The ENDOR spectrum of the radical in the reduced enzyme, shown in Figure 3B, is very similar to that reported for the anionic flavin radical in cholesterol oxidase.[28] In both cases, a pair of peaks which can be assigned to the C(6) proton (labeled c and c′ in Figure 3B) is located just inside those attributed to the methyl proton (d and d′). Although the hyperfine matrix for the C(6) proton is expected to be rhombic, only a single resonance is observed. Angle selected ENDOR spectra (not shown), obtained in the high-field ($g = 1.9998$) region, show that the peaks observed at 5.7 MHz for the radical under oxidizing conditions, and at 8.9 MHz under reducing conditions, both correspond to an out-of-plane hyperfine component and are likely close to one of the two in-plane components. ENDOR spectra of neutral radicals in solution exhibit a C(6) proton splitting[22,26] that is slightly smaller than that in the corresponding powder ENDOR (4 MHz versus 5.7 MHz), suggesting that the other in-plane component is ~1 MHz and is obscured by the strong matrix proton peaks. Thus, the hyperfine splitting that we observe for the C(6) proton, in both forms of the radical, is actually slightly larger than the true isotropic value.

The two C(1′) methylene protons are expected to be inequivalent as a result of twisting of the ribityl side chain. The proton having the smaller coupling (or larger value of θ in eq 1) is expected to have a splitting on the order of 1−2 MHz and is apparently obscured by the matrix region.[13] For the neutral radical, the methylene proton having the larger coupling is expected to be obscured by the C(8)-methyl splittings,[13] and is not readily seen. For the anionic form of the radical, we assign the peaks at 5.9 MHz (d and d′) to the larger of the splittings due to the two methylene protons. A smaller methylene splitting is expected for the anion radical form as demonstrated by the 33% decrease in the N(10)-methyl splittings observed for lumiflavin upon deprotonation (13.3 for the neutral form[20] and 8.9 for the anionic form[21,26]). As the hyperfine coupling of the methylene protons can be explained with a hyperconjugation model, a relatively smaller hyperfine coupling at the adjacent N(10) position would be expected in the deprotonated radical, and from the simulations of the cw spectra we find a 22% decrease in the N(10) hyperfine splitting (see below).

Close to the matrix regions we observe two pairs of peaks (marked e, e′ and f, f′ in Figure 3) whose splittings are both larger for the anionic form of the radical than for the neutral form. These peaks are mostly likely due to the C(9) proton and the C(7)-methyl protons.[26] Based upon the results of detailed substitution experiments which have been reported for lumiflavin,[26] we tentatively assign the larger of the two splittings to the C(9) proton.

A wider, 50 MHz, ENDOR frequency sweep is shown in Figure 4A (oxidized) and 4B (reduced). For the radical under oxidizing conditions, there are broad outlying features, labeled a and a′, with a coupling of 35 MHz, which are not seen under reducing conditions (Figure 4B). This splitting is attributable to the N(5) proton which is normally not observed in ENDOR spectra of flavins but is seen here, apparently because of the large magnetic field modulation used.

Analysis of X-Band and W-Band Spectra. Analysis of powder spectra of flavin radicals is complicated by the overlapping structure from two nitrogen atoms along with splittings arising from half-dozen or so protons. To simplify the simulation process we have employed several approaches. First, we have recorded first derivative spectra, that allow us to compute the second derivative spectra with both high resolution and high signal-to-noise, revealing much more resolved hyperfine structure. Second, we have used a multifrequency approach, recording both X-band and W-band spectra. This allows the separation of features, which are magnetic-field-dependent from those that are field-independent. Flavin radicals are typically studied by X-band EPR, but the use of W-band is very unusual; there is only one report: the W-band spectrum of a neutral flavin radical,[13] and only a minimal interpretation was given. Finally, we have used global ^{15}N isotope substitution to better distinguish the two large nitrogen splittings from the large N(5) proton splitting in the neutral form of the radical.

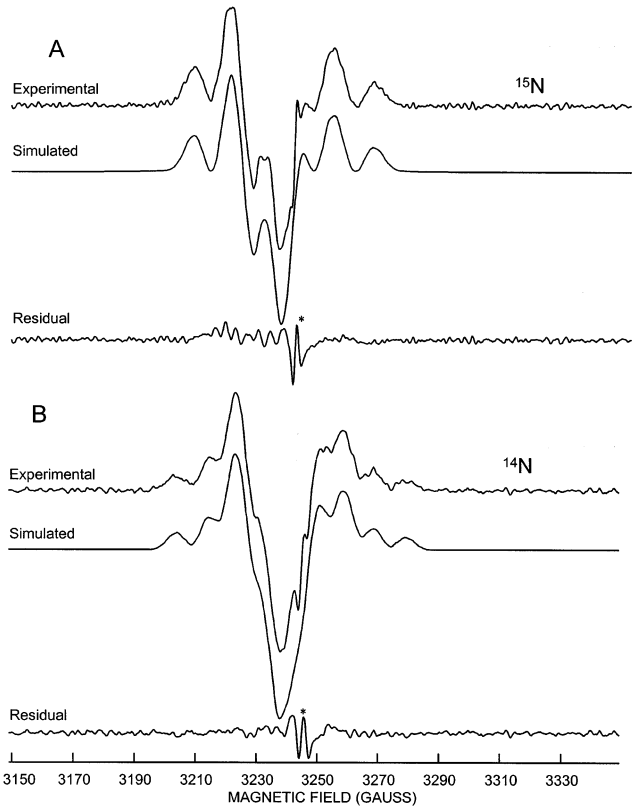

Figure 5. Second-derivative ($\partial^2\chi''/\partial B^2$) X-band spectrum of air-oxidized Na^+-NQR labeled with (A) and without (B) ^{15}N. Experimental spectra are shown in dark lines and simulated spectra in light. (Conditions were $T =$ 50 K, microwave power = 200 μW, field modulation 2 G ptp, $\nu_e = 9.083$ GHz, experimental time constant 0.032 s, and each spectrum was the average of 600 traces, each taking 30 s.)

Figures 5 and 6 show the second-derivative X-band and W-band spectra, respectively, together with simulations for both ^{14}N ($I = 1$, 99.63% naturally abundant) and ^{15}N ($I = 1/2$, >98%) labeled Na^+-NQR under oxidizing conditions. In simulating the spectra, we used several strategies to simplify the problem. First, the spectra were initially simulated individually until most features had been accounted for, and then all four spectra were fitted globally by minimizing the total square differences (TSD). Second, the nitrogen hyperfine matrices were assumed axial; lifting this restriction made no appreciable improvement in the TSD (less than 5% and less than 1 MHz change in hyperfine coupling constant). Third, the anisotropic splittings for the

(28) Medina, M.; Vrielink, A.; Cammack, R. *Eur. J. Biochem.* **1994**, *222*, 941−947.

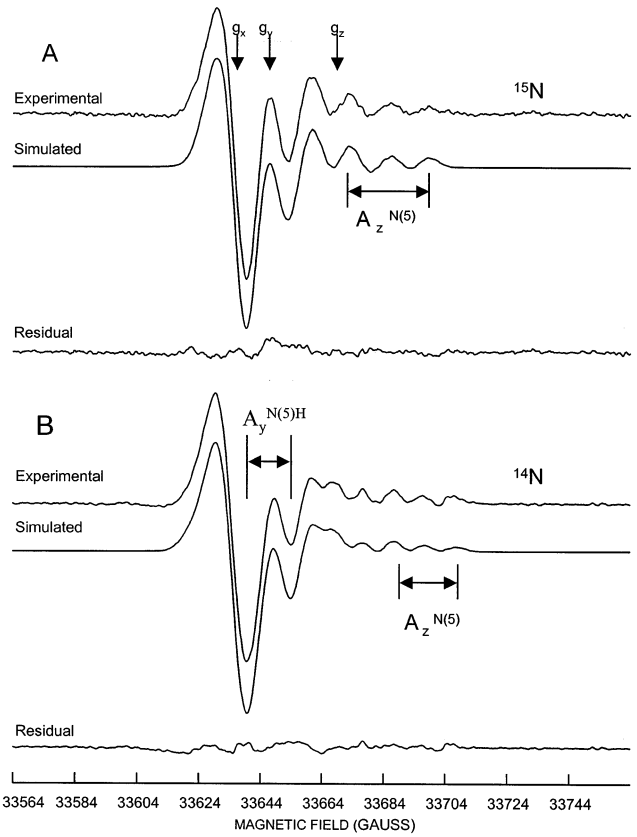

Figure 6. Second-derivative W-band spectrum of air-oxidized Na^+-NQR labeled with (A) and without (B) ^{15}N. Experimental spectra are shown in dark lines and simulated spectra in light lines. (Conditions were $T = 100$ K, microwave power $= 5$ μW, field modulation 2 G ptp, $\nu_e = 94.36$ GHz, experimental time constant 0.032 s, and each spectrum was the average of 1000 traces, each taking 30 s.)

methyl protons were taken directly from the ENDOR results. Additionally, the hyperfine splitting matrix of the C(6) proton was assumed to be nearly axial, with the two larger values being equated approximately to the observed ENDOR splittings. Based upon the arguments presented above, and theoretical calculations[29] of the anisotropic components for this proton, the third value was estimated to be about 1.4 MHz, with the other two couplings differing by about 0.6 MHz. For the C(1′) methylene proton having the larger coupling, the ENDOR splittings are obscured by the methyl proton splitting, and as such, the hyperfine couplings were initially set to 9 MHz and then allowed to vary in the final runs.

The additional splittings due to the C(9) and C(7)-methyl protons, the more weakly coupled C(1′) methylene proton, and the N(3) nitrogen are smaller than our spectral resolution of 2 G or 5.6 MHz, and as such are included by the use of an anisotropic Gaussian line shape pattern. An additional small Lorentzian component of 1 MHz was convoluted with the Gaussian line shape (Voight line shape) for all simulations except for the ^{15}N X-band simulation, which required 2 MHz. Contributions from A-strain, which arises from variations in the geometry around the atom, in particular that from the N(5) and C(1′) protons, are also expected to contribute to the residual line widths.

(29) Weber, S.; Möbius, K.; Richter, G.; Kay, C. W. M. *J. Am Chem. Soc.* **2001**, *123*, 3790−3798.

In addition to the principal values of the hyperfine matrices, some assumptions and strategies were used in determining the orientation of the matrices. For the orientation of the in-plane axes, the g_x-axis was initially assumed to be parallel to the *x*-axis of the N(5) and the C(1′) proton hyperfine matrices, aligned by the N(5)−H bond. The C(8)-methyl proton hyperfine matrix *x*-axis was assumed to be aligned by the C(8)−C(8α) bond and the C(6) proton hyperfine *x*-axis aligned by the C(6)−H bond. These assumptions worked well in simulating the spectra, with two exceptions: The g_x-axis needed to be rotated an extra 8° while the C(6) proton *x*-axis needed to be rotated by 30°. The large rotation of the latter is consistent with the large spin density expected at the nearby N(5) position. Initially, the assumption was made that the molecule was planar and that all matrices were collinear along the *z*-direction (normal to plane). This assumption worked well for simulation of the X-band spectra, but needed to be lifted in order to properly simulate the W-band spectra.

The X-band spectra in Figure 5 are very well accounted for by our simulations. The residuals for both the ^{14}N and ^{15}N spectral simulations show a signal in passage (χ') at $g = 2.0000$ which is attributable to the presence of a color center in the quartz sample tube. The weak multiplet structure seen in the residuals of the ^{15}N spectra, in the region where the absorption spectrum is strongest, is believed to be due, not to an impurity, but to differential saturation of the signal and is possibly attributable to differences in relaxation times for the ^{15}N- and ^{14}N-labeled radicals. (The amount of ^{15}N-labeled sample was limited, and for this reason the power was adjusted to optimize signal-to-noise ratio; this was a problem for X-band, but not for W-band, where 1/10 the amount of sample is required.)

In the W-band spectra (Figure 6) the upper or high-field half of the parallel region is removed or separated from the perpendicular region of the spectrum. This section of the parallel region shows a clear reduction in multiplicity upon labeling with ^{15}N; the shape of the parallel region is extremely well fitted by the simulation and the 3 G (8.5 MHz) methyl proton splitting is only barely resolved. The 16 G splitting in the low-field parallel region is due to the combined effect of the highly anisotropic N(5) proton hyperfine splitting and the rhombic **g**-matrix. This contrasts with an earlier report of the **g**-matrix of a neutral flavin radical as axial.[13] As mentioned earlier, the *z*-axes were initially assumed to be collinear. Lifting this restriction for the N(5), N(10), and N(5)H hyperfine matrices (those with significant anisotropy) led to an improvement of more than 50% in the SD, for both ^{14}N and ^{15}N W-band spectra, and greatly improved the fit to the low-field tail of the spectra. The largest noncoincidence between *z*-axes is that of the g_z-axis and the *z*-axis of the N(10) hyperfine matrix (13°, Table 2); the noncoincidence between the g_z-axis and the *z*-axis of the N(5) proton hyperfine matrix is smaller (5°). The effect of noncoincidence of the g_z-axes is better seen in the third-derivative spectra shown in Figure 7, where the low-field tail is properly accounted for only when the noncoincidence in the *z*-components is included. This low-field tail arises from what are known as off-axis extrema, which often occurs when a highly anisotropic hyperfine matrix is noncoincident with the **g**-matrix and is most often seen in the EPR spectra of square-planar copper complexes.[30] Also seen is the methyl proton hyperfine structure that is more easily resolved in the third-derivative spectra.

Table 2. Hyperfine Coupling Matrices (Principal Values in MHz) and **g**-Matrices for the Neutral and Anionic Flavin Radicals in Na^+-NQR Used in Simulations of X-band and W-band Spectra (Uncertainties in Parentheses)

	A_x	A_y	A_z	α^a	β^a	γ^a
			Neutral Radical			
^{14}N(5)[b]	0.2 (10)	0.2 (10)	52.5 (5)	45 (5)	7 (3)	
^{14}N(10)	2.0 (10)	2.0 (10)	28.9 (6)	12 (5)	13 (3)	
N(5)H	0.2 (10)	38.6 (6)	25.8 (6)	8 (5)	5 (3)	0 (3)
C(1′)H	8.1 (10)	9.3 (10)	8.4 (8)	8[f]	5[f]	0
C(8α)H	10.0[c]	8.5[c]	8.5[c]	8[f]	5[f]	−60
C(6)H	1.4[d]	5.4[d]	6.0[d]	8[f]	5[f]	30
W[e]	3.59	4.27	3.04	8 (5)		
G	2.004 25 (2)	2.003 60 (2)	2.002 27 (2)			
			Anionic Radical			
^{14}N(5)	2.3 (6)	2.3 (6)	57.6 (5)	21 (5)	1 (4)	
^{14}N(10)	1.6 (6)	1.6 (6)	22.8 (6)	1 (5)	6 (4)	
N(5)H						
C(1′)H	7.4 (8)	5.0 (8)	4.5 (6)	36 (5)	0	0
C(8α)H	11.9[c]	10.0[c]	10.0[c]	36[g]	0	−60
C(6)H	4.4[d]	8.9[c]	8.9[c]	36[g]	0	30
W[e]	4.49	2.09	3.48	54 (5)		
G	2.004 36 (2)	2.004 02 (2)	2.002 28 (2)			

[a] Euler angles relating the hyperfine matrix to the **g**-matrix, convention of Rose.[43] [b] For ^{15}N couplings, multiply by 1.403. [c] Values taken directly from ENDOR. [d] Values derived from ENDOR data. [e] Peak-to-peak Gaussian line width in Gauss. [f] Angles set equal to those for N(5)H. [g] Angles set equal to those for C(1′)H.

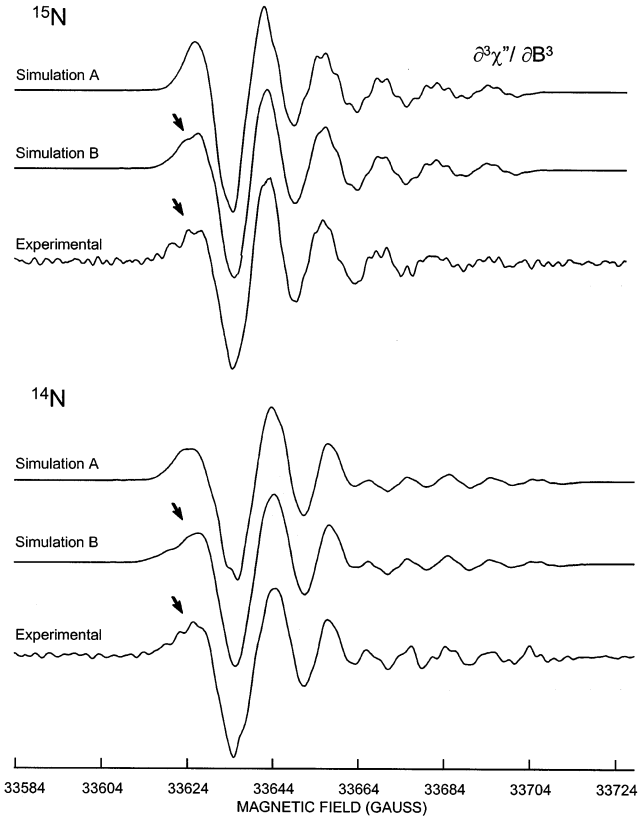

Figure 7. Third-derivative W-band spectra of air-oxidized Na^+-NQR labeled with and without ^{15}N labeling. Simulation A: Coincident *z*-axes; Simulation B: Noncoincident *z*-axes. (Generated from spectra shown in Figure 6.)

In simulating the radical spectrum in the reduced form of Na^+-NQR, the same assumptions and strategies were used as for the oxidized form. The lack of an N(5) proton coupling simplifies the analysis, and for this reason there was no need to obtain spectra of the reduced ^{15}N-labeled Na^+-NQR. The X-band spectrum (Figure 8) clearly shows the 3.6 G (10 MHz) splitting from the C(8)-methyl protons. Also seen is the nearly axial signal of the 2Fe−2S center (g = 2.0182, 1.9371, and 1.9316; 0.85:1 radical to 2Fe−2S center). The W-band spectrum (Figure 9) shows much less rhombic character than that of the neutral radical; the perpendicular region consists of a single peak and the parallel region is reduced in intensity as would be expected for a much more axial system. Even so, upon magnification, the parallel region shows the large, 20.5 G (57.5 MHz) splitting from the N(5) nitrogen and the 4.2 G (11.9 MHz) methyl splitting. Simulation parameters (Table 2) for the anionic radical generally follow the same pattern as those for the neutral radical, but with some noticeable differences. The rhombic character of the **g**-matrix is decreased by more than 50% and the in-plane noncoincidence is increased to 36°. The greatest out-of-plane noncoincidence is still between the **g**-matrix and N(10) hyperfine matrix, but the out-of-plane noncoincidence, in general, is smaller.

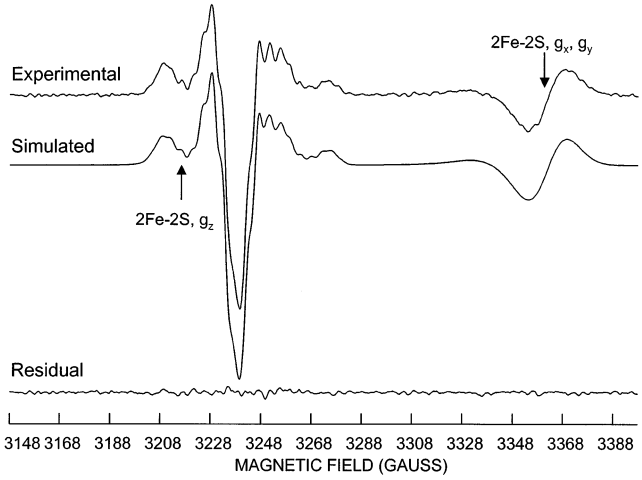

Figure 8. Second-derivative X-band spectrum of Na^+-NQR with reduced dithionite. Experimental spectra are shown in dark lines and simulated spectra in light. (Conditions were T = 50 K, microwave power = 63 μW, field modulation 2 G ptp, ν_e = 9.083 GHz, experimental time constant 0.032 s, and each spectrum was the average of 600 traces, each taking 30 s.)

(30) Pilbrow, J. R. *Transition Ion Electron Paramagnetic Resonance*; Clarendon Press: Oxford, 1990.

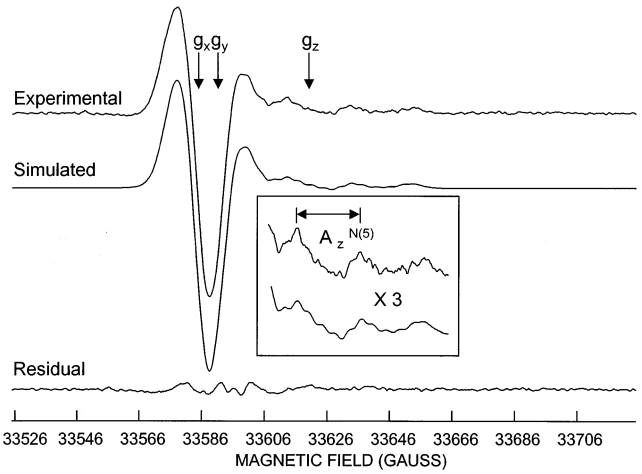

Figure 9. Second-derivative W-band spectrum of Na^+-NQR reduced with dithionite. Experimental spectra are shown in dark lines and simulated spectra in light lines. (Conditions were $T = 100$ K, microwave power = 16 μW, field modulation 2 G ptp, $\nu_e = 94.22$ GHz, experimental time constant 0.032 s, and each spectrum was the average of 1000 traces, each taking 30 s.)

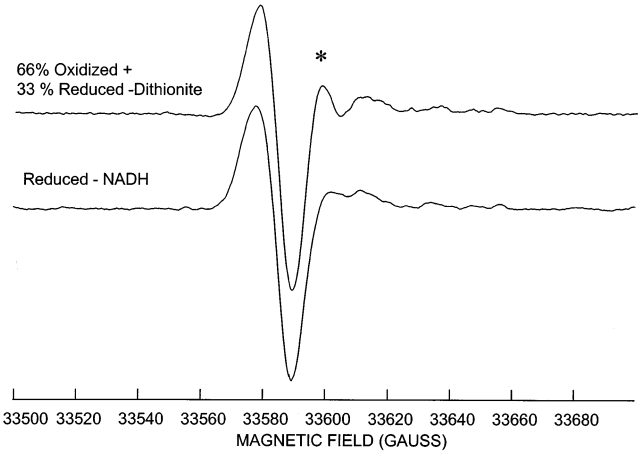

Figure 10. Second-derivative W-band spectrum of Na^+-NQR reduced with NADH compared to a composite spectrum generated by adding the spectrum of Na^+-NQR reduced with dithionite and that of air-oxidized Na^+-NQR in a 2:1 ratio.

Simulations thus show that the X-band and W-band spectra of the oxidized and dithionite-reduced enzyme can be accounted for by a single radical species (see Discussion). As mentioned earlier, the X-band spectrum of Na^+-NQR reduced with NADH appeared to be a 2:1 mixture of anionic and neutral radical. Figure 10 shows the measured W-band spectrum together with a spectrum obtained by adding the spectra of the air-oxidized and dithionite-reduced samples in a 2:1 ratio. The feature marked with an asterisk (*), in the calculated spectrum, is due to a combination of the N(5) proton splitting and rhombic **g**-matrix splitting and does not appear in, or is broadened out, in the spectrum of the NADH-reduced sample. The broadening of this feature could result from distribution of hyperfine couplings for the N(5) proton, i.e., A-strain.

Discussion

Nitrogen Hyperfine Coupling. We have been able to accurately measure differences in both the N(5) and N(10) nitrogen hyperfine matrices between protonated and deprotonated forms of the radical. For the neutral radical, the isotropic values ($A_{iso} = (A_x + A_y + A_z)/3$) of the N(5), N(10), and N(5)H hyperfine matrices (17.6, 11.0, and 21.5) agree well with the values reported (20.2, 10.1, and 21.6) for direct measurements from a highly resolved EPR spectrum of an aqueous deuterated FMN radical obtained by extraction from a fully deuterated flavoprotein.[31]

Values for the N(10) nitrogen hyperfine matrix of the neutral radical form also agree very well with those determined in ESSEM experiments.[32] A decrease in the N(10) hyperfine splitting is expected for the deprotonated radical,[23] and a 22% drop is observed here. This contrasts with reported ESSEM results, where identical N(10) hyperfine couplings have been found for both anionic and neutral flavin radicals.[32] For the N(10) nitrogen hyperfine coupling, we find the ratio of A_z to A_{iso} to be 2.6, which is close to the traditionally accepted value of 2.5.[21] For the N(5) hyperfine splitting this ratio is found to be much larger, especially in the case of the neutral radical, where it is almost 3.0. The larger values of this ratio can be attributed to the higher spin density, particularly in the case of the neutral radical, which is expected at the C4a position.[23] While contributions from the spin density on the adjacent C4a position to the anisotropic (dipolar) part of the nitrogen hyperfine splitting will add in-phase, the contribution to the isotropic (spin polarized) part of the nitrogen hyperfine splitting will add out-of-phase.

Shift in Spin Density upon Deprotonation. The EPR and ENDOR results both reveal a decrease in the N(10) nitrogen and C(1′) proton hyperfine splittings, and an increase in the N(5) nitrogen and the C(8), C(6), C(9), and C(7α) proton hyperfine splittings upon removal of the N(5) proton. This corresponds to a decrease in the spin density at the N(10) position upon deprotonation and an increase in spin density, both at the N(5) position and on the aromatic ring. This, and the relatively larger splittings at positions ortho and para to the N(5) position in the anion radical, suggest that, upon deprotonation, there is a shift in spin density from the conjugated semiquinoneimine system (N10−C10a−C4a−C4−O4) to the aminobenzene system (N(5) and the aromatic ring). This contraction in spin density is also consistent with the observed change from blue to red color seen upon deprotonation of flavin radicals.[23,33] [Note: The actual color of the enzyme (yellow/oxidized, pale brown/reduced) is determined primarily by the flavins and the 2Fe−2S center. While a blue to red color change is not observed here, a loss in the absorption peak at 460 nm due to the neutral radical in the optical spectrum is observed upon reduction of the enzyme.[4]]

Noncoincidence of Hyperfine and g-Matrices. Analysis of W-band spectra shows that the flavin radical, in particular in the neutral form, is nonplanar. We find the greatest out-of-plane noncoincidence is between the **g**-matrix and the N(10) hyperfine matrix, a smaller noncollinearity is between the *z*-components of the **g**-matrix and the N(5) hyperfine matrix, and a minimal noncoincidence is between the **g**-matrix and the N(5)H hyperfine matrix (see Figure 11). While the isoalloxazine ring is usually expected to be nearly planar, there can also be a significant puckering at or folding around the N(5) and N(10) positions

(31) Crespi, H. L.; Norris, J. R.; Katz, J. J. *Biochim. Biophys. Acta* **1971**, *253*, 509−513.
(32) Martínez, J. I.; Alonso, P. J.; Gómez-Moreno, C.; Medina, M. *Biochemistry* **1997**, *36*, 15526−15537.
(33) Massey, V.; Palmer, G. *Biochemistry* **1966**, *5*, 3181−3189.

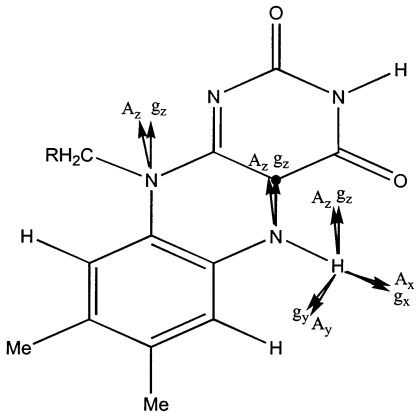

Figure 11. Orientation of the N(10), N(5), and N(5)H hyperfine matrices relative to the **g**-matrix for the protonated flavin radical. The orientation of the axes of the **g**-matrix is assumed to be directed by the N(5)−H and C(4)−O bonds.

giving a so-called butterfly structure.[34] From X-ray crystal structure models (Protein Data Bank of the Research Collaboratory for Structural Bioinformatics) of a 173 flavoprotein containing FMN, we have calculated the N(5)−N(10)−C(1′) angle, and find a mean angle of 174.9° with a standard deviation of 5.4°. Thus, the nonplanar character of the isoalloxazine ring can vary significantly. Almost all structures are of FMN in the oxidized form, but the X-ray structure of a flavin semiquinone has been characterized for one system, flavodoxin.[35,36] In this system the isoalloxazine ring shows only a minimal distortion with a N(5)−N(10)−C(1′) angle of 178.8°. From these results a nearly planar structure for the isoalloxazine ring would be expected, although a nonplanar ring structure cannot be ruled out.

Rhombic Character of g-Matrices. The **g**-matrix for the flavin radical depends primarily upon the distribution of spin density in the p_z orbitals of the flavin heteroatoms and the in-plane bonding around those heteroatoms, in particular, the presence of in-plane nonbonding orbitals. For the flavin radical, the primary contributions will be from the spin density on the O(4), N(5), and N(10) atoms. Because the spin−orbit coupling for oxygen (150 cm^{-1}) is roughly twice that of nitrogen (70 cm^{-1}), the **g**-matrix will be especially sensitive to spin density at the O(4) position, a position that is normally blind to conventional X-band EPR as ^{16}O has a nuclear spin of zero and therefore does not give rise to hyperfine structure. The small increase of 15% in the axial component ($(g_x + g_y)/2$) of the **g**-matrix upon deprotonation is much smaller than the factor of 2 or more that is reported for a benzosemiquinone radical.[37] This suggests that the expected increase in the *g*-shift due to the addition of a nonbonding orbital at the N(5) position is partially canceled by a decrease in the spin density at the O(4) position, the contribution of which is proportionally larger because of the larger spin−orbit coupling for oxygen. A significant decrease in the rhombic component of the **g**-matrix is observed upon deprotonation. Considering the contribution from the O(4) position alone, the largest component of the **g**-matrix will be along the C(4)−O(4) bond or along the bisector of the two nonbonding orbitals (as is seen for phenoxyl radicals such as the tyrosyl radical[38]). In the present case, for the neutral flavin radical, where neither the N(5) or N(10) positions have nonbonding orbitals, the orientation of the in-plane *g*-axes should be determined primarily by the contribution from the O(4) atom and, as expected, we find the g_x-axis to be closely aligned to the C(4)−O(4) bond. In the case of the anionic radical, the N(5) position will have one nonbonding orbital, and the largest component of the **g**-matrix will be normal to the plane containing the p_z orbital and the in-plane nonbonding orbital. The asymmetry around the N(5) atom, with its one nonbonding orbital, is the reverse of that at the O(4) atom, with its two nonbonding orbitals, so that the largest component of the in-plane **g**-matrix for the N(5) contribution will be rotated 90° in the aromatic plane from that of the O(4). Thus, a shift of some of the spin density from the O(4) atom to the N(5) atom will result in a decrease in the rhombic character of the **g**-matrix (a complete transfer of spin density would cause a reversal of the ordering of g_x and g_y.)

Table 3. Comparison of Experimental Hyperfine Couplings for the $CH_3(8)$ and H(6) Protons in Neutral and Anionic Flavin Radical Enzyme Cofactors (in MHz) Obtained from ENDOR Spectra

flavin/system	C(8α)H[a]	C(6)H[b]	ref
Neutral Flavins			
DNA photolyase from *E. coli*	7.49	4.86	13
glucose oxidase, pH 5.9	7.5		21
FAD in H_2O pH 6.5	7.8		21
ferredoxin-$NADP^+$ reductase	8.12	5.11	44
flavodoxin from *Azotobacter vinelandii*	8.3	5.5	22
flavodoxin from *Megashaera elsdenii*	8.5	5.6	22
4-hydroxybutyryl-CoA dehydratase	8.5	6.23	45
chorismate synthase	8.58	6.3	46
Na^+-NQR−oxidizing conditions	9.1	5.7	this work
Anionic Flavins			
riboflavin or FAD in H_2O, pH 12	9.5		21
Na^+-NQR−reducing conditions	10.7	8.9	this work
cholesterol oxidase	10.9	9	28
glucose oxidase, pH 9.8	11.0		21

[a] Calculated isotropic splitting. [b] Observed splitting.

Polarizability and Shifts in Spin Density. Changes in the hyperfine splitting of the C(8)-methyl protons and the C(6) proton, particularly for the neutral flavin radical, have been attributed to changes in solvent polarity around the flavin in the protein.[29] For the radical in the oxidized form of Na^+-NQR, the C(8)-methyl splitting is the largest such splitting reported so far for a neutral flavin radical (Table 3). While one could attribute this to a markedly hydrophilic environment, we believe that this is oversimplified for several reasons. First, the methyl splittings for the Na^+-NQR radical, like those in many other flavoprotein systems, are already larger than those observed for flavin radicals in water alone (see Table 3). Second, there is not always a one-to-one correlation between changes in the C(8)-methyl splitting and the C(6) proton splitting. In the case of DNA photolyase, both C(8)-methyl and C(6) proton splittings are relatively small, and this has been attributed to the hydrophobic environment around the flavin.[29] For the Na^+-NQR radical, only the methyl splitting is overly large, while the 5.7 MHz C(6) proton splitting is fairly typical for a neutral flavin radical. This suggests that some change in the microenvironment

(34) Zheng, Y.; Ornstein, R. L. *J. Am. Chem. Soc.* **1996**, *118*, 9402−9408.
(35) Ludwig, M.; Pattridge, K. A.; Metzger, A. L.; Dixon, M. M.; Eren, M.; Feng, Y.; Swenson, R. P. *Biochemistry* **1997**, *36*, 1259−1280-.
(36) Hoover, D. M.; Ludwig, M. L. *Protein Sci.* **1997**, *6*, 2525−.
(37) Burghaus, O.; Plato, M.; Rohrer, M.; Möbius, K.; MacMIllan, F.; Lubitz, W. *J. Phys. Chem.* **1993**, *97*, 7639−7647.
(38) Bleifuss, G.; Kolberg, M.; Potsch, S.; Hofbauer, W.; Bittl, R.; Lubitz, W.; Graslund, A.; Lassmann, G.; Lendzian, F. *Biochemistry* **2001**, *40*, 15362−15368.

around the radical is causing the shift in spin density to the C(8) position. In particular, coupling, or bonding to the protein, of the N(5) proton and other heteroatom groups on the pyrimidine ring, such as O(1), N(3), and O(4), is expected to polarize the bonds at the heteroatom positions, pulling electron charge density to the lower right portion of the isoalloxazine ring (as drawn in Scheme 1) and pushing electron spin density in the opposite direction toward the upper right of the isoalloxazine ring. This is supported by theoretical calculations[29] that show, when hydrogen bonding of a flavin radical to amino acid fragments is taken into consideration, there is a decrease in spin density in the lower half of the benzene ring, namely the C(6) and C(7) positions, and an increase in the upper half at C(8) and C(9).

Origin of the Flavin Radical. Na^+-NQR contains a total of four flavins: a noncovalently bound FAD in subunit F, two covalently bound FMNs in subunits B and C, and a noncovalently bound riboflavin in an unknown location.[7−9,39] The two covalently bound flavins are attached to threonine residues by phosphodiester linkages.[8] This is highly unusual, since covalently attached flavins have been found previously to be linked to the protein only at the C(8) or the C(6) positions on the isoalloxazine ring.[26] Redox titrations of Na^+-NQR[4] show the presence of one $n = 1$ component, attributable to the reduction of the 2Fe−2S center, and three $n = 2$ components, attributable to the reduction of three flavins. Because the aromatic system of the flavinsemiquinone does not extend significantly beyond the C(1′) position on the ribityl side chain, it is difficult, based solely upon the analysis of hyperfine couplings, to assign the Na^+-NQR radical as originating from either FAD, FMN, or riboflavin. We have found that the flavin radical EPR signal remains if either the noncovalently bound FAD (Zhou et al., manuscript in preparation) or the FMN in subunit C (Barquera et al., unpublished results) is removed; thus, the covalently bound FMN in subunit B and the noncovalently bound riboflavin are the only two cofactors that could be responsible for the radical signals.

The finding that a flavin radical is observed in near stoichiometric (1:1) amounts in both the oxidized and reduced forms of the enzyme indicates that either (1) upon reduction of the enzyme the original flavin semiquinone becomes reduced to the flavohydroquinone form, while a second flavin cofactor is reduced from the flavoquinone to the semiquinone form, replacing one flavin radical with another, or (2) the signals arise from a single flavin cofactor with a near infinite semiquinone formation constant relative to the flavoquinone and flavohydroquinone forms.

The first of these models would place severe constraints on the redox properties of the two flavins. The neutral and anionic radicals appear in relatively pure form in the oxidized and dithionite-reduced enzyme. In the NADH-reduced enzyme, the EPR signal represents a mixture of neutral and anionic radicals, but the overall amplitude of this mixed signal is not significantly different from that in the oxidized enzyme. This indicates that, if there are two different radicals, the midpoint potential for the semiquinone to flavohydroquione transition, $E_{sq/hq}$, of the anionic flavin must be very close to the midpoint potential for the flavoquinone to semiquinone transition, $E_{ox/sq}$, of the neutral flavin, since a difference of 60 mV would be enough to cause a 50% change in the sum of amplitudes in the crossover region. Because the anionic radical is at or near stoichiometric concentrations even in the presence of a 400-fold excess of dithionite, $E_{sq/hq}$ for the anionic radical must be much less than −660 mV, the midpoint potential of dithionite.[40] As the signal of the neutral radical is not affected by either solvent isotope substitution or changes in pH, the flavin would have to be isolated from protonic exchange with the external medium, but not necessarily from electron transport. Alternatively, the single flavin model would require a cofactor with an extremely stable semiquinone, which is converted from the neutral to the anionic form when the enzyme becomes reduced. This flavin would have to be isolated from the external medium, but would still need to be able to exchange protons with some other redox cofactor in the enzyme. Isolation of the radical also from electron transport might explain some of the stability of the radical but is not a requirement. As such, the observation that the neutral radical is affected by excess NAD^+ is compatible with both models, but would slightly favor the two-radical model.

Radical Stability. While near stoichiometric concentrations of flavin radicals have been found in many flavoprotein systems, the flavin radical species is usually not intrinsic to the system but must be generated by photoreduction or chemical reduction of the resting form and readily disappears upon reoxidation of the protein.[33] In Na^+-NQR, a signal from a flavin radical is found in near stoichiometric concentrations, in both the resting (air-oxidized) and reduced states of the enzyme. These EPR signals are unaffected by changes in pH and do not respond to solvent deuterium exchange. As such, Na^+-NQR is unlike any other flavoprotein reported to date. The observed stability of flavin radicals in typical protein systems has been attributed to binding to the protein, in much the same way that binding to Zn^{2+} stabilizes these and other semiquinone radicals.[41] A neutral flavin radical would be stabilized by binding to a negatively charged amino acid, while an anionic flavin radical would be stabilized by binding to a positively charged amino acid. However, if a single flavin cofactor is responsible for both forms of the Na^+-NQR radical, this semiquinone must be highly stabilized in both neutral and anionic forms. A few proteins, for example, glucose oxidase, exhibit flavin radicals, which can exist in both neutral and anionic forms. To explain this, it has been suggested that hydrogen bonding of N(5) to a histidine group occurs.[27] Binding of Na^+ to the anionic radical could also result in a stabilization of this radical for the same reasons that Zn^{2+} can do. While thermodynamic stabilization of the flavin radical in Na^+-NQR may well exist, the lack of interaction of the radical with the external aqueous environment could also play a significant role in stabilizing the radical.

Role of Flavin Radical in Na^+-NQR. Regardless of whether the neutral and anionic radical signals in Na^+-NQR arise from one or two flavins, a flavin semiquinone could play a role in the translocation of sodium ions by the enzyme. If the radical is due to a single flavin, although this flavin does not participate directly in redox chemistry, its protonation state must still be affected by changes in the redox state of the enzyme. The

(39) (a) Zhou, W.; Bertsova, Y. V.; Feng, B.; Tsatsos, P.; Verkhovskaya, M. L.; Gennis, R. B.; Bogachev, A. V.; Barquera, B. *Biochemistry* **1999**, *38*, 16246−16252. (b) Barquera, B.; Zhou, W.; Morgan, J. E.; Gennis, R. B. *Proc. Natl. Acad. Sci. U.S.A.* **2002**, *99*, 10322−10329.

(40) Mayhew, S. G. *Eur. J. Biochem.* **1978**, *85*, 535−547.

(41) Müller, F.; Eriksson, L. E. G.; Ehrenberg, A. *Eur. J. Biochem.* **1970**, *12*, 93−103.

reversible loss of the N(5) proton upon reduction of the enzyme would be unique for a flavoenzyme system. In this case, it is likely that some other center in the enzyme, when reduced, is able to abstract a proton from the radical. It is not yet clear how far away from the radical this center would be, and what electron- or proton-conducting pathways would connect them. With the loss of a proton from a neutral radical, the uptake of a compensating cation would be expected. Similarly, if two flavins are involved, formation of the anionic radical by addition of an electron might also call for a compensating positive charge. In either case, this cation would most likely be Na^+. No ^{23}Na ($I = 3/2$) superhyperfine is seen in the spectrum of the reduced enzyme, but the splitting would be expected to be only a few megahertz, at most, as has been observed for *o*-benzosemiquinone anion radicals.[42] Simulation of the spectrum of the reduced Na^+-NQR that includes ^{23}Na hyperfine coupling gives an upper limit of 2 MHz, which would be indistinguishable in the present measurements.

Conclusions

We have unequivocally shown that the radical observed in the air-oxidized form (resting state) of Na^+-NQR is a neutral flavin semiquinone, while in the reduced enzyme the radical is an anionic flavin semiquinone, deprotonated at the N(5) position. In the case of the enzyme reduced by NADH, an intermediate form is observed, consistent with a partially deprotonated radical, whereas when a large excess of dithionite is used, an essentially completely deprotonated radical is observed. The magnitude of proton splittings suggests strong hydrogen bonding or coupling of the radical with the protein. Of the four flavin cofactors in the enzyme, only two could potentially give rise to these signals: the covalently bound FMN in subunit B and the noncovalently bound riboflavin. Work is underway to establish whether the radical signals arise from two different flavins or from one stable radical which becomes deprotonated upon reduction of the enzyme, and to determine which cofactor or cofactors are involved.

By combining results of ENDOR and multifrequency cw EPR, an essentially complete determination of the **g**-matrix and all major nitrogen and proton hyperfine matrices has been made for both the neutral and anionic forms of the radical. This is the first time the full **g**-matrix of a flavin radical has been determined. In the neutral radical, the **g**-matrix has significant rhombic character, but this is significantly decreased in the anionic radical. We believe that the noncoincident out-of-plane component of the **g**-matrix and nitrogen hyperfine matrices are a result of puckering of the pyrazine ring.

Acknowledgment. This research was supported by NIH Grants, RR01811 (IERC), GM 35103 (C.P.S.), and HL16011 (R.B.G.).

JA0207201

(42) Pedersen, J. A. *Handbook of EPR Spectra from Quinones and Quinols*; CRC Press: Boca Raton, FL, 1985.
(43) Rose, M. E. *Elementary Theory of Angular Momentum*; Wiley: New York, 1957.
(44) Medina, M.; Gómez-Moreno, C.; Cammack, R. *Eur. J. Biochem.* **1995**, *227*, 529−536.
(45) Çinkaya, I.; Buckel, W.; Medina, M.; Gómez-Moreno, C.; Cammack, R. *J. Biol. Chem.* **1997**, *378*, 8433−8849.
(46) Macheroux, P.; Petersen, J.; Borenemann, S.; Lowe, D. J.; Thorneley, R. N. F. *Biochemistry* **1996**, *35*, 1643−1652.